Interactions of Cold- and Warm-Core Rings with Environmental Shear

DORON NOF AND CHUAN SHI

Department of Oceanography, The Florida State University, Tallahassee, Florida

(Manuscript received 4 May 1988, in final form 26 December 1988)

ABSTRACT

A two-layer analytical model of cold- and warm-core rings has been constructed to explore steady interactions of isolated eddies with horizontally sheared flows around and below the eddies. Steady inviscid solutions to the quasi-geostrophic equations are found by assuming that the environmental shear is weak compared to the ring's shear.

It is found that such interactions lead to elliptical rings; in contrast to our expectations, *the eccentricity of the rings is caused solely by the lower layer shear and is independent of the surrounding upper shear.* Namely, when there is no shear in the lower layer, the ring's shape is circular, even though there may exist a surrounding upper shear. When the flow inside the ring rotates in the same direction as the lower shear, the elliptical ring is aligned along the lower layer flow. On the other hand, when the flow inside the ring rotates in the opposite direction to that of the lower shear, the elliptical ring is aligned across the lower-layer flow.

Surprisingly, when the surrounding upper flow shear rotates in the opposite direction to that of the flow below the ring, a chain of weak vortices is generated outside the ring in the upper layer. This chain of vortices is a result of trapped planetary waves. When the surrounding upper flow and the lower layer flow rotate in the same sense, there are no such ambient vortices. Instead, U-turned flows on both sides of the ring are established.

Possible applications of this theory to both warm- and cold-core rings are mentioned.

1. Introduction

When a circular (warm- or cold-core) ring is placed in a sheared flow, distortions in its shape are generated due to the distorted pressure fields. Such a situation is created when an environmental shear is suddenly imposed on a circular ring that is initially embedded in a resting ocean or when, during its formation, the ring is injected into a flow field with preexisting shear. Our aim in this paper is to compute the ring's distortions and the influence of the ring on the surrounding fluid. As described below, variations of this classical problem have been addressed by various investigators during the past decade.

The general computations are quite difficult because of two aspects. First, the position of the ring's edge is unknown and must be determined as a part of the solution (Figs. 1 and 2). Namely, the matching of the ring flow to the external flow must be done along a free separating streamline whose position and shape are not known a priori. Second, the interactions of the ring and its surroundings are essentially nonlinear. We shall see that, despite these aspects, it is possible to isolate some steady solutions. To derive these solutions we shall linearize the governing equations using a perturbation scheme in ϵ, the ratio of the exterior shear to the ring's shear. Specifically, we shall focus on quasi-geostrophic flows with a weak shear *both underneath and around the eddies.*

a. Previous investigations

For a general review of isolated eddies studies the reader is referred to Flierl (1987). Distortions in circular eddies due to stability and other time-dependent processes were addressed by Spence and Legeckis (1981), Mied and Lindemann (1983), Cushman-Roisin et al. (1985), Cushman-Roisin (1986, 1987), Young (1986), Send (1986), McCalpin (1987), and Melander et al. (1987). Distortions that are more directly related to our present investigation—those resulting from the interaction between eddies and environmental shears—are listed in Table 1. While those studies are informative, they do not specifically address the problem where a ring is affected by both an upper and lower shear which is considered in our study.

b. Methods

Our mathematical treatment includes the following steps. First, the Bernoulli equation and potential vorticity equation are derived by specifying the ring's potential vorticity and the upper upstream shear. Second, the full Bernoulli equation and the potential vorticity equation are scaled and simplified by a perturbation scheme in ϵ which represents both the ratio of the environmental shear to the ring's shear and the ring's

Corresponding author address: Professor Doron Nof, Department of Oceanography, Florida State University, Tallahassee, FL 32306-3048.

TABLE 1. A summary of theoretical studies of eddies interactions with environmental shear (f is the Coriolis parameter, β its gradient, and H the upper-layer undisturbed depth).

Model type	Number of active regions in the model	Continuous properties across the ring's edge	Cauase of the ring's distortion	Reference
Purely barotropic (H = const), f = 0, analytical	2	Streamfunction and tangential velocity	Surrounding shear and strain	Moore and Saffman (1972) Kida (1981)
Purely barotropic (1982) (H = constant), f-plane, analytical	2	Streamfunction and tangential velocity	Surrounding flow	Swenson
Two-layer lens-like warm ring, f-plane, analytical	2	Pressure	Lower-layer shear	Nof (1985)
Two-layer lens-like warm ring, f-plane, analytical	2	Pressure	Lower-layer shear or strain	Ruddick (1987)
Two-layer Jovian vortex, β-plane, numerical	3	Streamfunction, potential vorticity and pressure	Not specifically identified	Ingersoll and Cuong (1981)
Two-layer cold and warm rings, f-plane, analytical	3	Streamfunction and pressure	Lower-layer shear	Present study

intensity. This perturbation analysis reduces the governing equations to quasi-geostrophic equations with a weak external shear. Third, we derive one governing equation with one unknown by substituting the Bernoulli equation into the potential vorticity equation. Finally, the resulting Bessel-type equation is solved analytically.

This study is organized as follows. The formulation of the problem is presented in section 2, and the perturbation analysis in section 3. The detailed solutions are obtained in section 4, and a special solution is given in section 5. The results are discussed in section 6 and the major points of this study are summarized in section 7.

2. Formulation

Consider again the two-layer model shown in Figs. 1 and 2. The upper layer has uniform density ρ and the lower layer has slightly larger density ($\rho + \Delta\rho$). Our model is steady, frictionless, nondiffusive and hydrostatic. The origin of the polar coordinate (r, θ) is located at the center of the eddy, and the coordinate rotates (uniformly) with angular velocity $f/2$ about the vertical axis. The lower layer flow's direction is $\theta = 0$.

Conceptually, we view the distorted ring as being the result of the adjustment of a circular ring to the application of external shear. Our attention is given to the final steady state reached after the adjustment is completed. The resulting ring is bounded by a closed free streamline and has uniform potential vorticity (f/D, where D is the cylinder initial depth). The velocity of the infinitely deep lower layer, U_l, and the upstream upper-layer speed, U_u, are,

$$U_l = -Ar\sin\theta, \quad 0 \leqslant r < \infty \tag{2.1a}$$

$$U_u = -Er\sin\theta, \quad r \to \infty \tag{2.1b}$$

where A and E are given. Note that when A is not equal to E, there is a vertical gradient of vorticity in the environmental fluid. The model has three active regions: the ring, the upper exterior with the upstream linear shear, and the infinitely deep lower layer with linear shear everywhere.

The lower-layer shear and the upper exterior shear are taken to be weak compared to the ring's shear. Namely, as a result of the shear, the ring is a slightly distorted circle so that the edge position can be expanded in a Taylor series,

$$r = r_0 + \epsilon^{1/2} r_1(\theta) + \epsilon r_2(\theta) + \cdots, \quad \epsilon^{1/2} \ll 1 \tag{2.2}$$

where ϵ corresponds to the square of the ratio between the environmental shear to the ring's shear (B). For convenience, ϵ has been defined here as the square of the epsilon in Nof (1985). Note that B is the shear that the ring would have at its edge ($R = r_0$) in the absence of a lower layer shear.

a. General structure of governing equations

Since our problem involves two parameters that are weak—the exterior flow and the ring's intensity—it is necessary to derive the equations from first principles. In polar coordinates, the potential vorticity and Bernoulli equations for the upper layer flow are

$$\frac{\nabla[(\nabla\psi)/h] + f}{h} = P(\psi); \quad \nabla = \mathbf{e}_r \frac{\partial}{\partial r} + \frac{\mathbf{e}_\theta}{r}\frac{\partial}{\partial\theta} \tag{2.3}$$

$$\frac{1}{2}\left(\frac{\nabla\psi}{h}\right)^2 + g'(h - H) + \frac{1}{2} fAr^2\sin^2\theta = G(\psi) \tag{2.4}$$

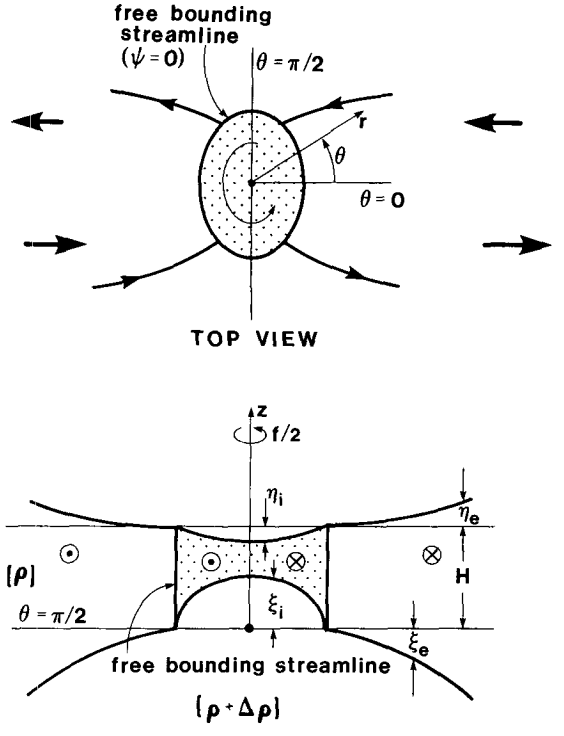

FIG. 1. A schematic diagram of the model under study. The ring [bounded by a free streamline, $r = r_0 + \epsilon r_1(\theta)$] is stationary on an f-plane and is assumed to have a uniform potential vorticity. Away from the ring ($r \to \infty$), the lower layer and the upper exterior are assumed to have two independent linear shears. Hence, there are three active regions: the ring (shaded), the upper exterior, and the lower layer. As a result of the interactions with ambient shears, the ring's shape is distorted and the ambient field is modified by the ring.

where h, H, g', $P(\psi)$ and $G(\psi)$ correspond to the total depth of the upper layer, the undisturbed depth of the upper layer, the reduced gravity ($g\Delta\rho/\rho$), the potential vorticity function and the Bernoulli function, respectively. Here, ($\mathbf{e}_r$, $\mathbf{e}_\theta$) are the unit vectors in polar coordinates, $P(\psi) = dG(\psi)/d\psi$, and the streamfunction is defined by

$$hv_r = -\frac{1}{r}\partial\psi/\partial\theta, \quad hv_\theta = \partial\psi/\partial r \tag{2.5}$$

where $\psi = 0$ corresponds to the edge of the ring and v_r and v_θ are the horizontal velocity components in polar coordinates (Fig. 1). The last (pressure) term on the left hand side of (2.4) is due to the lower layer shear. This term couples the upper and the lower layer. The specific structure of the governing equations for the ring and the environment is to be determined by $P(\psi)$ and $G(\psi)$, which will be derived in the next subsection.

b. Governing equations for the ring

Without loss of generality, we may specify the uniform potential vorticity of the ring to be

$$P_i(\psi_i) = (1 + \mathrm{Ro})f/H \tag{2.6}$$

where $\mathrm{Ro}(= B/f)$ is the (given) Rossby number of the ring. The subscript i indicates that the variable in question is associated with the ring (upper interior). The corresponding Bernoulli function is

$$G_i(\psi_i) = (1 + \mathrm{Ro})f\psi_i/H \tag{2.9}$$

where, for convenience, we have let G_i ($\psi_i = 0$) $= 0$. Substitution of (2.6) and (2.9) into (2.3) and (2.4) provides the complete potential vorticity and Bernoulli equations for the ring.

c. Governing equations for the exterior

The potential vorticity and Bernoulli functions of the upper exterior are determined from the geostrophic upstream condition at infinity,

$$h_e = H + f(E - A)r^2 \sin^2\theta/2g', \quad r \to \infty \tag{2.10}$$

$$\psi_e = [H/2 + f(E - A)r^2 \sin^2\theta/8g']Er^2 \sin^2\theta, \quad r \to \infty \tag{2.11}$$

where, in accordance with our previous notation, the subscript e denotes variables of the upper exterior. Application of (2.10) and (2.11) to (2.3) and (2.4) gives

$$P_e(\psi_e) = \frac{g'E(E + f)}{[(g'H)^2E^2 + 2g'fE(E - A)\psi_e]^{1/2}} \tag{2.12}$$

$$G_e(\psi_e) = \frac{E + f}{f(E - A)} \times \{[(g'H)^2E^2 + 2g'fE(E - A)\psi_e]^{1/2} - g'HE\} \tag{2.13}$$

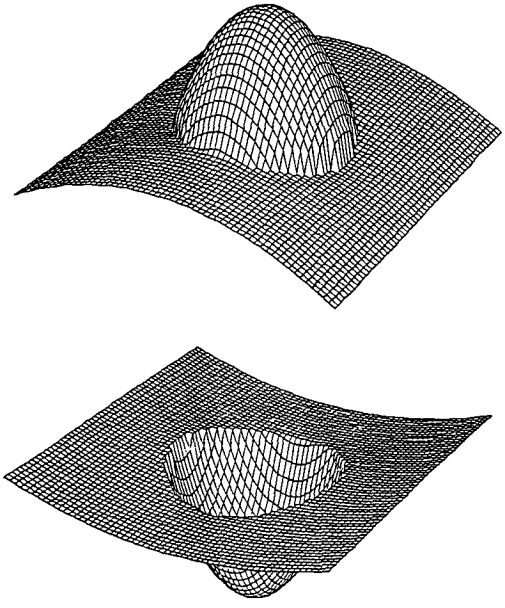

FIG. 2. A schematic three-dimensional view of the interfaces for a cold ring (upper panel) and a warm ring (lower panel) interacting with environmental shear.

which satisfies $P_e(\psi_e) = dG_e(\psi_e)/d\psi_e$, as should be the case. Substitution of (2.12) and (2.13) back into (2.3) and (2.4) gives the complete potential vorticity and Bernoulli equations for the upper exterior.

d. Boundary conditions

The boundary and matching conditions are

$$h_i(r, \theta) = h_e(r, \theta); \quad r = r_0 + \epsilon^{1/2} r_1(\theta) + \cdots \tag{2.14a}$$

$$\psi_i(r, \theta) = \psi_e(r, \theta); \quad r = r_0 + \epsilon^{1/2} r_1(\theta) + \cdots \tag{2.14b}$$

$$\partial\psi_i/\partial r = \partial\psi_i/\partial\theta = 0, \quad r = 0 \tag{2.14c}$$

$$\psi_e = (1/2)HEr^2 \sin^2\theta, \quad r \to \infty. \tag{2.14d}$$

The first and second conditions [(2.14a) and (2.14b)] state that the pressure and streamfunction are continuous across the ring's edge. [Recall that the streamfunction is defined to be zero along the ring's edge (Fig. 1)]. The third condition (2.14c) states that the velocity components in the r and θ directions are zero at the center of the eddy and the last condition (2.14d) reflects the uniform upstream shear (E).

Note that we do not require the tangential velocity to be continuous across the ring's edge. This is because, in free streamline theory (Batchelor 1967; Garabedian 1964; Milne-Thompson 1960), an inviscid fluid is allowed to have a velocity front (i.e., discontinuity of velocity). Similarly, a potential vorticity front may exist across the ring's edge. It is appropriate to point out that, strictly speaking, requiring the velocity to be continuous across the free separating streamline *over-constrains the problem.* Some investigators (e.g., Swenson 1982) prefer to have such a continuous speed but, because the system is now over constraint, the imposed structure of some other parameters in the problem (e.g., the vorticity) must be relaxed. The argument that the velocity needs to be continuous in order for the solution to be stable is not entirely valid because, in the actual fluid, friction will smooth the discontinuity. In other words, in the most general case, one needs to include the frictional terms if the velocity is to be continuous and the problem is not to be over constraint. This is not to say that it is wrong to require the velocity to be continuous across the separating streamline (in an inviscid model) *but by doing so one limits the actual freedom of the ring to adjust to the surrounding environment.* Consequently, solutions such as those of Swenson (1982) correspond to rather special circumstances.

3. Perturbation analysis

a. Nondimensionalization

The following dimensionless variables are introduced:

$$\psi^* = \psi/\mathrm{Ro} f R_d^2 H, \quad \xi^* = \xi/\mathrm{Ro} H,$$
$$P^* = P/(f/H), \quad G^* = G/g'H$$
$$r^* = r/R_d, \quad \epsilon^{1/2} = A/B, \quad \mathrm{Ro} = \alpha\epsilon,$$
$$\alpha = B^3/fA^2, \quad R = E/A \tag{3.1}$$

where $R_d\,[=(g'H/f^2)^{1/2}]$ is the internal deformation radius, α is a transformed parameter (introduced for convenience), and R is the ratio of the upper-layer shear (E) to the lower-layer shear (A). For mathematical tractability, we shall focus our attention on situations where,

$$\epsilon \ll 1; \quad \mathrm{Ro} \sim O(\epsilon); \quad \alpha \sim O(1); \quad R \sim O(1);$$
$$P^* \sim O(1); \quad G^* \sim O(1); \quad B \sim O(\epsilon f),$$
$$E \sim O(A) \sim O(\epsilon^{3/2} f); \quad \psi_i^* \sim O(1);$$
$$\xi_i^* \sim O(1); \quad \psi_e^* \sim O(\epsilon^{1/2}); \quad \xi_e^* \sim O(\epsilon^{1/2}). \tag{3.2}$$

With this scaling both the ring and the exterior are quasi-geostrophic (because both the Rossby number and the amplitude are small). The ring's intensity (B) is small [$O(\epsilon)$] and the upper exterior shear is even smaller [$O(\epsilon^{3/2})$]; the lower-layer shear is of the same order as the upper-layer shear.

b. Perturbation expansion

It is further assumed that, for the ring and upper exterior, the streamfunctions and interfacial displacements can be expanded in power series, e.g.,

$$\psi_i^*(x^*, y^*, \epsilon) = \psi_i^{(0)}(x^*, y^*) + \epsilon^{1/2}\psi_i^{(1)}(x^*, y^*) + \cdots \tag{3.3a}$$

$$\xi_i^*(x^*, y^*, \epsilon) = \xi_i^{(0)}(x^*, y^*) + \epsilon^{1/2}\xi_i^{(1)}(x^*, y^*) + \cdots \tag{3.3b}$$

$$\psi_e^*(x^*, y^*, \epsilon) = \epsilon^{1/2}\psi_e^{(1)}(x^*, y^*) + \epsilon\psi_e^{(2)}(x^*, y^*) + \cdots \tag{3.3c}$$

$$\xi_e^*(x^*, y^*, \epsilon) = \epsilon^{1/2}\xi_e^{(1)}(x^*, y^*) + \epsilon\xi_e^{(2)}(x^*, y^*) + \cdots. \tag{3.3d}$$

We shall see that with these expansions and (3.2), the zeroth-order problem corresponds to the quasi-geostrophic regime considered by Csanady (1979). The external shear enters the first-order problem whereas the nonlinear square of the velocity in the Bernoulli invariant enters higher-order approximations which are beyond the scope of this study.

By substituting (3.3) into the nondimensional form of the governing equations, we find the zeroth-order equations and boundary conditions for the ring:

$$\nabla^2\psi_i^{(0)} = 1 + \xi_i^{(0)}, \tag{3.4a}$$

$$\xi_i^{(0)} = \psi_i^{(0)}, \tag{3.4b}$$

and

$$\frac{\partial \psi_i^{(0)}}{\partial r^*} = 0, \quad r^* = 0 \tag{3.5a}$$

$$\psi_i^{(0)} = 0, \quad r^* = r_0^* \tag{3.5b}$$

where the derivation of the second boundary condition (3.5b) involved a Taylor expansion around $r^* = r_0^*$. Similarly, the first-order relations are

$$\nabla^2 \psi_i^{(1)} = \xi_i^{(1)}, \tag{3.6a}$$

$$\xi_i^{(1)} = \psi_i^{(1)} - (r^*)^2 \sin^2\theta/2 \tag{3.6b}$$

$$\frac{\partial \psi_i^{(1)}}{\partial r^*} = \frac{\partial \psi_i^{(1)}}{\partial \theta^*} = 0, \quad r^* = 0 \tag{3.7a}$$

$$\psi_i^{(1)} + r_1^*(\theta)\left(\frac{\partial \psi_i^{(0)}}{\partial r^*}\right) = 0, \quad r^* = r_0^* \tag{3.7b}$$

where, as before, a Taylor expansion around $r^* = r_0^*$ has been used to obtain the second boundary condition (3.7b). Note that we can eliminate $\xi_i^{(0)}$ to obtain one equation (with one unknown) for the ring's zeroth-order problem, and we can eliminate $\xi_i^{(1)}$ and get one equation (with one unknown) for the ring's first-order problem.

Similarly, we obtain the first-order equations for the upper exterior,

$$\nabla^2 \psi_e^{(1)} + (1 - 1/R)\psi_e^{(1)} = R + \xi_e^{(1)} \tag{3.8a}$$

$$\xi_e^{(1)} = \psi_e^{(1)} - (r^*)^2 \sin^2\theta/2. \tag{3.8b}$$

Again, elimination of $\xi_e^{(1)}$ provides an equation with one unknown ($\psi_e^{(1)}$) for the upper exterior. The resulting equation is subject to the boundary conditions,

$$\psi_e^{(1)} = 0, \quad r^* = r_0^* \tag{3.9a}$$

$$\psi_e^{(1)} = \frac{1}{2} R(r^*)^2 \sin^2\theta, \quad r^* \to \infty \tag{3.9b}$$

As before, condition (3.9a) has been obtained from (2.14) by using a Taylor series expansion around $r^* = r_0^*$.

4. Solution

To solve the coupled problem relating the ring and its upper exterior, one first needs to find a general solution for the ring and another for its upper exterior. Then, one matches these two solutions along the ring's edge and thus obtains the detailed solutions. As stated earlier, the matching conditions are continuity of streamfunction and upper-layer depth. It is important to realize that, for quasi-geostrophic motions such as ours, the continuity of the upper-layer depth (or pressure) across the ring's edge is *automatically satisfied* since the square of the velocity in the Bernoulli equation is negligible, *so that the upper-layer depth is a linear function of the streamfunction.* [This can be easily verified by examining (3.4b), (3.6b), and (3.8b).] Consequently, we can acquire the ring's solution and the upper exterior's solution by matching the streamfunction alone.

a. Detailed solution for the ring (interior)

The zeroth-order solution of (3.4) satisfying (3.5a) is identical to the solution derived by Csanady (1979). The only difference between the solution presented below and Csanady's (1979) analysis is that Csanady has "pushed" his solution beyond the range of parameters that is strictly allowed in the quasi-geostrophic approximation (Flierl 1979) whereas we shall keep our variables within the permitted range. The solution consists of a sum of a particular solution and a homogeneous one, i.e.,

$$\psi_i^{(0)} = -1 + \sum_{n=0}^{\infty} I_n(r^*)(a_n \cos n\theta + b_n \sin n\theta) \tag{4.1}$$

where $I_n(r^*)$ are the modified Bessel functions of the first kind. The boundary condition (3.5b) requires that

$$a_0 = \frac{1}{I_0(r_0^*)}, \; a_n = 0, \quad \text{if} \quad n = 1, 2, 3 \cdots$$

$$b_n = 0, \quad \text{for all } n \tag{4.2}$$

Hence, the zeroth-order solution is

$$\psi_i^{(0)} = \frac{I_0(r^*) - I_0(r_0^*)}{I_0(r_0^*)}. \tag{4.3}$$

By inspection, we find the first-order solution of (3.8) satisfying (3.7) to be

$$\psi_i^{(1)} = \tfrac{1}{2}(r^*)^2 \sin^2\theta + 1 \tag{4.4a}$$

$$r_1^* = -\left[\frac{1}{2}(r^*)^2 \sin^2\theta + 1\right]\left[\frac{I_0(r_0^*)}{I_1(r_0^*)}\right]. \tag{4.4b}$$

By adding the zeroth-order solution (4.3) and the first-order solution (4.4), the total solution for the upper interior can be written as

$$\boxed{\psi_i^* = \frac{I_0(r^*) - I_0(r_0^*)}{I_0(r_0^*)} + \epsilon^{1/2}\left(1 + \frac{1}{2} r^{*2} \sin^2\theta\right) + O(\epsilon).} \tag{4.5}$$

The corresponding interfacial displacement (ξ_i^*), and the position of the edge [$r^*(\theta)$] is

$$\boxed{\xi_i^* = \frac{I_0(r^*) - I_0(r_0^*)}{I_0(r_0^*)} + \epsilon^{1/2} + O(\epsilon)} \tag{4.6a}$$

$$r^* = r_0^* + \epsilon^{1/2}\left[\frac{1}{2}(r^*)^2\sin^2\theta + 1\right] \times \left[\frac{I_0(r_0^*)}{I_1(r_0^*)}\right] + O(\epsilon). \quad (4.6b)$$

Note that to $O(\epsilon^{1/2})$, ψ_i^* depends on θ whereas ξ_i^* does not. This is a result of the lower layer pressure which alters the usual quasi-geostrophic relationship between ξ_i^* and ψ_i^* [see (3.6b)].

We define the ring's eccentricity (e) to be

$$e = (a - b)/a \quad (4.7)$$

where a, b are the lengths of the ellipse along and across the lower layer flow. Using our solution we find,

$$e = \frac{\epsilon^{1/2} r_0^*}{2}\frac{I_0(r_0^*)}{I_1(r_0^*)} + O(\epsilon). \quad (4.8)$$

It is important to note that the surrounding upper shear (E) does not enter the solution for the ring! Namely, the ring's shape is influenced solely by the lower-layer shear; it is independent of the upper layer shear. We shall return to this point later.

b. Detailed solution for the upper exterior

We shall first address the case where $R = E/A > 0$. In this case, the flow in the upper exterior rotates in the same direction as that of the lower layer. The solution of (3.8) satisfying (3.9a) consists again of a sum of a particular solution and a homogeneous solution,

$$\psi_e^{(1)} = \frac{1}{2}R(r^*)^2\sin^2\theta + \sum_{n=0}^{\infty} K_n\left(\frac{r^*}{R^{1/2}}\right) \times (c_n\cos n\theta + d_n\sin n\theta), \quad R > 0 \quad (4.9)$$

where $K_n(r^*/R^{1/2})$ are the modified Bessel functions of the second kind.

By considering (3.9b), we can determine c_n and d_n

$$c_0 = \frac{R(r_0^*)^2}{4K_0(r_0^*/R^{1/2})}, \quad c_2 = \frac{R(r_0^*)^2}{4K_2(r_0^*/R^{1/2})}$$

$$c_n = 0, \quad \text{if } n = 1, 3 \text{ or larger}; \quad d_n = 0, \quad \text{for all } n. \quad (4.10)$$

Hence, (4.9) can be written as

$$\psi_e^{(1)} = \frac{R(r_0^*)^2}{4}\frac{K_0(r^*/R^{1/2})}{K_0(r_0^*/R^{1/2})} + \frac{R(r_0^*)^2}{4}\frac{K_2(r^*/R^{1/2})}{K_2(r_0^*/R^{1/2})}\cos 2\theta + \frac{1}{2}R(r^*)^2\sin^2\theta, \quad R > 0 \quad (4.11)$$

and the total solution for the upper exterior is

$$\psi_e^* = \epsilon^{1/2}\left\{\frac{1}{4}R(r_0^*)^2\left[\frac{K_2(r^*/R^{1/2})}{K_2(r_0^*/R^{1/2})} - \frac{K_0(r^*/R^{1/2})}{K_0(r_0^*/R^{1/2})}\right] - \frac{1}{2}R(r_0^*)^2 \times \left[\frac{K_2(r^*/R^{1/2})}{K_2(r_0^*/R^{1/2})} - \frac{(r^*)^2}{(r_0^*)^2}\right]\sin^2\theta\right\} + O(\epsilon), \quad R > 0 \quad (4.12)$$

The corresponding interfacial displacement is

$$\xi_e^* = \epsilon^{1/2}\left\{\frac{1}{4}R(r_0^*)^2\left[\frac{K_2(r^*/R^{1/2})}{K_2(r_0^*/R^{1/2})} - \frac{K_0(r^*/R^{1/2})}{K_0(r_0^*/R^{1/2})}\right] - \frac{1}{2}R(r_0^*)^2 \times \frac{K_2(r^*/R^{1/2})}{K_2(r_0^*/R^{1/2})}\sin^2\theta\right\} + \frac{1}{2}(R-1)(r^*)^2\sin^2\theta + O(\epsilon), \quad R > 0. \quad (4.13)$$

We shall now proceed and consider the solution for $R = E/A < 0$. In this case, the flow in the upper exterior rotates in the *opposite direction* to that of the lower layer. After similar calculation, we find

$$\psi_e^* = \epsilon^{1/2}\left\{\frac{1}{4}Rr_0^{*2}\left[\frac{J_2(r^*/|R|^{1/2})}{J_2(r_0^*/|R|^{1/2})} - \frac{J_0(r^*/|R|^{1/2})}{J_0(r_0^*/|R|^{1/2})}\right] - \frac{1}{2}Rr_0^{*2} \times \left[\frac{J_2(r^*/|R|^{1/2})}{J_2(r_0^*/|R|^{1/2})} - \frac{(r^{*2})}{(r_0)}\right]\sin^2\theta\right\} + O(\epsilon); \quad R < 0 \quad (4.14)$$

where $J_n(r^*/|R|^{1/2})$ are Bessel functions of the first kind. The corresponding interfacial displacement is

$$\xi_e^* = \epsilon^{1/2}\left\{\frac{1}{4}R(r_0^*)^2\left[\frac{J_2(r^*/|R|^{1/2})}{J_2(r_0^*/|R|^{1/2})} - \frac{J_0(r^*/|R|^{1/2})}{J_0(r^*/|R|^{1/2})}\right] - \frac{1}{2}R(r_0^*)^2\frac{J_2(r^*/|R|^{1/2})}{J_2(r_0^*/|R|^{1/2})}\sin^2\theta\right\} + \frac{1}{2}(R-1)(r^*)^2\sin^2\theta + O(\epsilon), \quad R < 0. \quad (4.15)$$

For large r^*, the upper exterior solutions for $R > 0$, (4.12) and the upper exterior solution for $R < 0$, (4.14) can be approximated by

$$\psi_e^* = \frac{1}{2}\epsilon^{1/2}R \times \left\{(r^*)^2 - (r_0^*)^{5/2}\frac{\exp[(r_0^* - r^*)/R^{1/2}]}{(r^*)^{1/2}}\right\}\sin^2\theta + O(\epsilon), \quad R > 0, \quad r^* \gg 1$$

$$\psi_e^* = \frac{1}{2}\epsilon^{1/2}R \times \left[(r^*)^2 - \frac{(r_0^*)^{5/2}}{(r^*)^{1/2}}\frac{\cos(r^*/|R|^{1/2} - \pi/4)}{\cos(r_0^*/|R|^{1/2} - \pi/4)}\right]\sin^2\theta + O(\epsilon), \quad R < 0, \quad r^* \gg 1.$$

These expressions indicate that when the lower layer shear A rotates in the opposite direction to the upstream shear of the upper layer (i.e., $R = A/E < 0$), the perturbation of the streamfunction ψ_e^* decays slowly (as $\sim 1/(r^*)^{1/2}$) and is a sinusoidal function of r^*. On the other hand, when the lower-layer shear A rotates in the same sense as the upper layer shear E (i.e., $R = A/E > 0$), the perturbation of the streamfunction ψ_e^* decays uniformly and rapidly [according to $-\exp(r^*/R^{1/2})/(r^*)^{1/2}$].

The streamlines for $R > 0$ and $R < 0$ are shown in Figs. 3 and 4, respectively, and the eccentricity in Fig. 5. In both Figs. 3 and 4 the ring is elliptical due to the underlying shear. The manner in which the shear affects the ring is shown in Fig. 6; it is similar to the process discussed by Nof (1985) in the sense that the shear underneath the ring simply adds to (or subtracts from) the swirl of the ring. Recall that, as stated earlier, the surrounding upper layer shear has no effect on the ring.

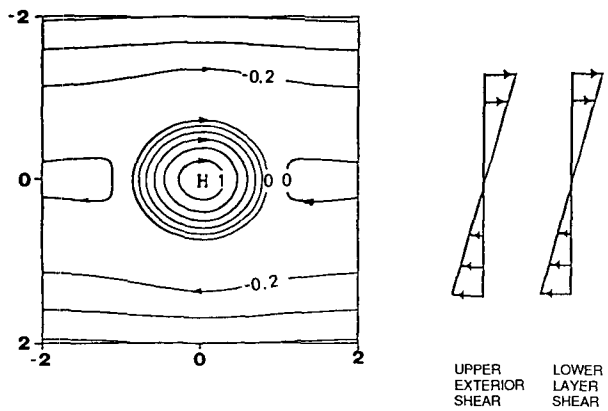

FIG. 3. Typical streamfunctions of a warm-core ring and its upper exterior for $R > 0$. On the right are the lower layer shear and the upper exterior shear at infinity; these two shears rotate in the same sense. The major axis of the anticyclonic eddy is aligned with the lower layer shear. There are U-turned streamlines on both sides of the ring. The parameters are: $\epsilon = 0.01$; $r_0 = R_d$; $R = 0.8$.

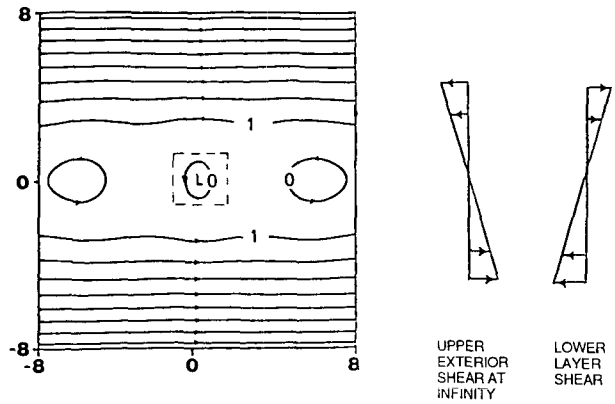

FIG. 4a. Typical streamfunctions of a cold-core ring and its upper exterior for $R < 0$. On the right are the lower layer shear and the upper layer shear at infinity; these two shears rotate in opposite directions. Note that the shear in the lower layer is anticyclonic so that the cyclonic eddy lies across the lower layer flow. Interactions between active regions generate a chain of vortices upstream and downstream ($\epsilon = -0.01$; $r_0 = R_d$; $R = -0.8$). A close-up of the area bounded by the dashed line is shown in Fig. 4b, and a wide-angle view in Fig. 4c.

Of course, this is only true to the order of approximation that we have solved for. Higher order approximations will certainly include such an effect.

As far as the surrounding exterior is concerned, when $R > 0$ (Fig. 3) there are simply U-turned flows on the two sides of the ring. In contrast, when $R < 0$ (Fig. 4), chains of vortices are generated on the two sides of the ring; these chains of vortices correspond to trapped planetary waves. The difference between the two cases can be explained as follows. When the flow in the two environmental layers is in the same sense ($R > 0$), the planetary waves generated by the interaction of the ring and the environment (due to the sloping interface) are swept away (Fig. 3). By contrast, when the shear in the two environmental layers is in the opposite sense the waves are trapped by the flow (Fig. 4). In a way, the above process is similar to the one encountered in

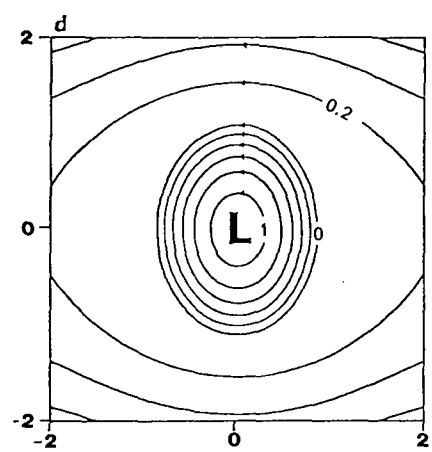

FIG. 4b. A close-up of the ring shown in Fig. 4a.

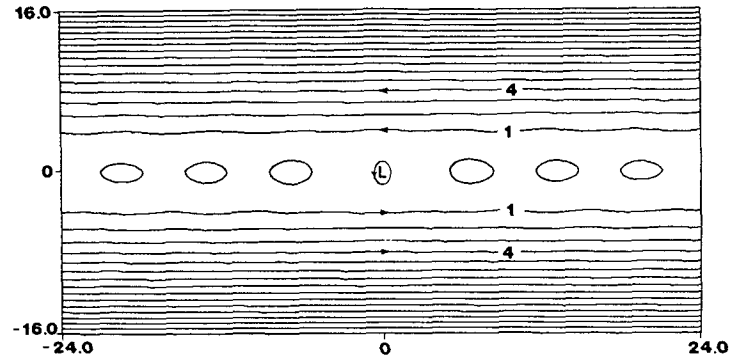

FIG. 4c. A wide-angle view of the interaction shown in Fig. 4a. Note that the interactions between active regions generate a chain of vortices upstream and downstream.

flow over topography (e.g., see McCartney 1975). In that case, eastward flows over topography on a β plane can have stationary waves because the flow is directed toward the east whereas the Rossby waves move westward so that the net movement can be zero. On the other hand, westward flows can never have stationary waves because both the flow and the Rossby waves are directed westward. In our case, isolated vortices are generated upstream and downstream of the central ring because there is flow in both directions. This suggests that there is rather active interaction between the ring and its environment.

The above analysis completes our general solution to the problem. It is instructive to also examine the special case of no-flow in the lower layer; this is done in the next section.

5. The special case of no-flow in the lower layer ($A = 0$)

For this special case we need to redefine our small parameter ϵ and rescale the equations because (3.1) breaks down. Specifically, we define a new small parameter, $\mu = E/f$. Also, we redefine

$$\mathrm{Ro} = B/f; \quad \psi^* = \psi/\mathrm{Ro} f R_d^2 H; \quad \xi^* = \xi/\mathrm{Ro} H \quad (5.1)$$

where $\mu \ll 1$; $\mathrm{Ro} \sim O(\mu)$; $\psi^* \sim O(1)$; $\xi^* \sim O(1)$; $E/B \sim O(1)$. As before, we expand all variables in a power-series in μ,

$$\psi_e^* = \psi_e^{(0)} + \mu\psi_e^{(1)} + \cdots; \quad \psi_i^* = \psi_i^{(0)} + \mu\psi_i^{(1)} + \cdots. \quad (5.2)$$

The zeroth-order quasi-geostrophic equations for the interior and exterior are

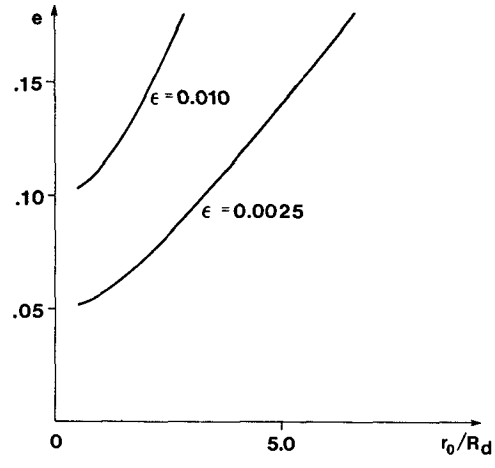

FIG. 5. The eccentricity (e) versus the dimensionless undisturbed radius r_0/R_d. Note that the eccentricity increases as the undisturbed radius increases. Also, note that the eccentricity is independent of the surrounding upper layer shear (see text).

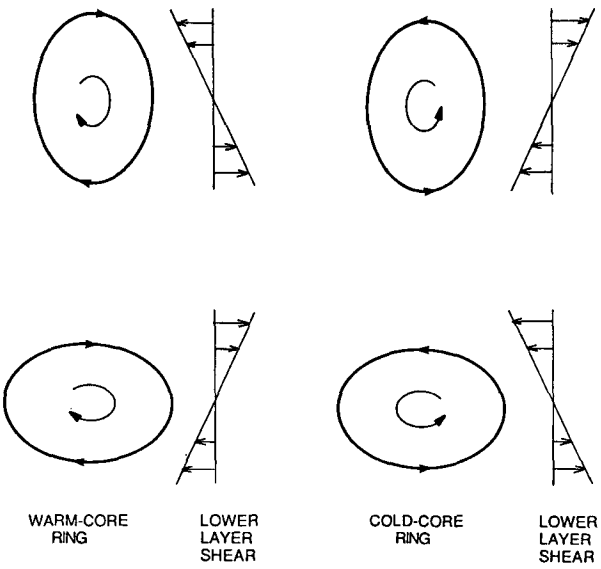

FIG. 6. A schematic diagram of the ring's structure in the presence of lower-layer shear. When the flow inside the ring rotates in the opposite direction to that of the lower layer, the ellipse is perpendicular to the lower layer flow (upper left and right). In contrast, when the flow inside the ring rotates in the same sense as the lower layer shear, the ellipse is oriented along the lower layer flow (lower left and right).

$$\nabla^2\psi_i^{(0)} = 1 + \xi_i^{(0)}, \quad \xi_i^{(0)} = \psi_i^{(0)} \tag{5.3}$$

$$\nabla^2\psi_e^{(0)} = E/B, \quad \xi_e^{(0)} = \psi_e^{(0)}. \tag{5.4}$$

The corresponding boundary conditions are

$$\psi_e^{(0)} = \psi_i^{(0)}, \quad r^* = r_0^* \tag{5.5a}$$

$$\frac{\partial\psi_i^{(0)}}{\partial r^*} = \frac{\partial\psi_i^{(0)}}{\partial\theta} = 0, \quad r^* = 0 \tag{5.5b}$$

$$\psi_e^{(0)} = \frac{E(r^*)^2\sin^2\theta}{2B} - \frac{E(r_0^*)^2}{4B}, \quad r^* \to \infty \tag{5.5c}$$

where the last term on the right hand side of (5.5c) has been added for convenience.

The solution is

$$\boxed{\psi_i^* = \frac{I_0(r^*)}{I_0(r_0^*)} - 1 + O(\mu)} \tag{5.6a}$$

$$\boxed{\psi_e^* = \frac{E}{2B}\left[(r^*)^2 - \frac{(r_0^*)^4}{(r^*)^2}\right]\sin^2\theta + \frac{E}{4B}(r_0^*)^2\left[\frac{(r_0^*)^2}{(r^*)^2} - 1\right] + O(\mu).} \tag{5.6b}$$

Note that, in contrast to the general cases discussed in section 4 where the exterior flow enters the first-order problem, here the exterior solution enters the zeroth-order problem. This solution is shown in Fig. 7 which indicates that, *when the lower shear is relaxed and the flow is quasi-geostrophic, the ring remains circular.*

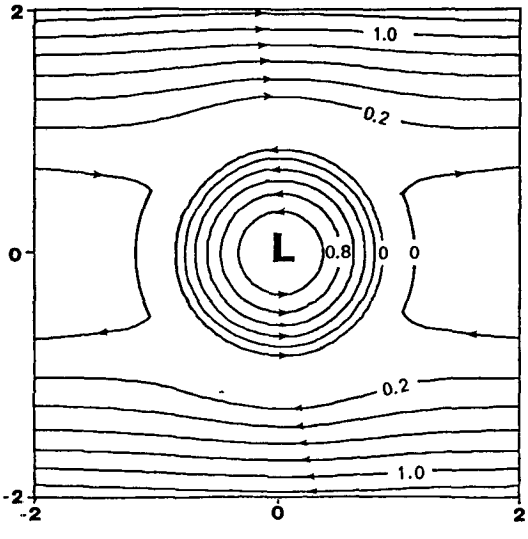

FIG. 7. Streamfunctions of the ring and its upper exterior for $A = 0$. The lower layer is motionless so that the ring is circular despite the surrounding shear ($r_0 = R_d$, $E = -0.6B$).

6. General remarks

a. Relationship to Swenson (1982) model

As mentioned earlier, Swenson (1982) investigated a ring surrounded by a shear using a purely barotropic (H = const) model on an f-plane. His governing equations are similar to ours, but the boundary conditions are very different. In both formalisms, the continuity of streamfunction across the ring's edge is used. However, although the continuity of pressure across the ring's edge is automatically satisfied by the quasi-geostrophic equations, Swenson also matched the tangential velocity across the ring's edge, arguing that such a match assures the continuity of pressure. Since such a match is actually *guaranteed* for quasi-geostrophic motions, from a mathematical point of view the additional conditions over-restrict the system. As a direct result of this nonslip condition, Swenson (1982) found that a distortion could be caused by a surrounding shear.

It is argued here that in Swenson's case the communication between the exterior and the ring is much more severe than it should be and that, as a result, the ring is distorted. We contend that, for quasi-geostrophic motions, one should not match the velocity unless friction is included. As mentioned, such a treatment shows that weak exteriors cannot alter the ring's shape (Fig. 7).

b. Relationship to other studies

In the appropriate limits, our study is in qualitative agreement with the analytical investigations of Nof (1985) and Ruddick (1987) for lenslike eddies. (Recall that the Nof (1985) and Ruddick (1987) cases are strongly nonlinear so that they cannot be quantitatively compared to our present study.) It is also in qualitative agreement with the numerical study of Ingersoll and Cuong (1981) for cold and warm rings, as should be the case. For a detailed discussion the reader is referred to Shi (1988).

c. Possible applications

At this stage a quantitative comparison to observations is very difficult because of the limited available data. Many observations suggest that both warm- and cold-core rings are elliptical but we do not have sufficient information on the environmental flow to meaningfully compare it with our model. For example, Fig. 8 illustrates that cold-core ring BOB was elliptical and that, in contrast to the process discussed by Spence and Legeckis (1981), it did not rotate in time. This suggests that its ellipticity may be related to an underlying shear of the kind previously discussed. However, a close examination of relevant observations reveals that the deep circulation pattern (Hogg 1983) is very complicated and does not correspond to a simple shear structure. Also, during the observations of Vastano et al. (1980),

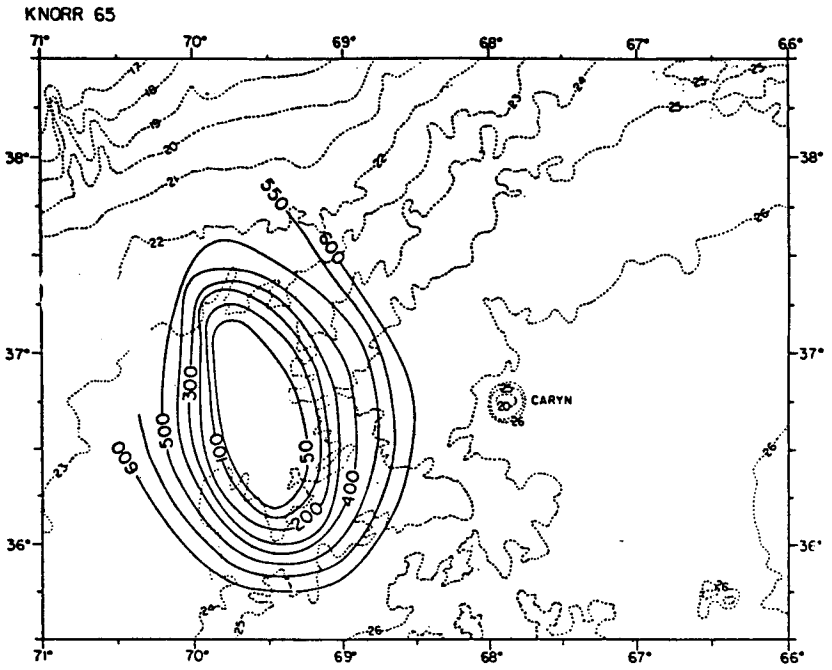

FIG. 8. Contoured depth (m) of the 15°C isotherm from ring BOB during 15–16 April 1977. Bottom topography from NAVOCEANO bathymetric charts (in fathoms $\times 10^{-2}$. Adapted from Vastano et al. (1980).

the ring interacted with the Gulf Stream suggesting that other processes were probably active in the area. Similar statements can be made regarding the observations of Kelley and Weatherly (1985) and Lewis and Kirwan (1987), both of whom observed elliptical warm rings. Presently, we do not have enough information to isolate the cause of the ellipticity. We can, however, say that our model points to a mechanism that might be responsible for the ellipticity of rings. It is hoped that future observational programs will look into the environment of eddies more closely so that a meaningful comparison can be made.

Finally, a comment should be made on the importance of steering currents. Such currents were discussed in Nof (1985). It has been stated there that steering currents merely advect the lens; they have no influence on the shape of the lens. A careful analysis of the present problem of eddies with a finite depth along the rim indicates, however, that, for such eddies, this is not necessarily the case. In fact, the integrated methods used by Nof (1983a) to find the migration rate do not yield any information in the present case. It appears that the role of advection in the problem at hand is considerably more complicated than that in Nof (1985) and it is, therefore, left as a subject for further investigation.

d. Finite lower layer

The assumption of infinitely deep lower layer is quite restrictive because, in reality, it may contain relatively strong motions. As shown in Nof (1983b) and Shi (1988), the assumption is valid as long as $f\xi/H_l \ll E$, where ξ is the interface displacement, E the exterior shear and H_l is the lower-layer depth.

7. Summary

A two-layer analytical model has been developed for examining the flow field of a cyclonic or anticyclonic ring (and its adjacent upper exterior) responding to the presence of upper and lower shear at infinity. The model has three active flow regions: the ring, the upper exterior, and the infinitely deep lower layer (Figs. 1, 2). The coupling between these three regions depends solely on the continuity of streamfunction and pressure across the two-layer's interface and the ring's edge. This f-plane model has been developed under the following assumptions: 1) the flow is frictionless, nondiffusive and steady; 2) the ring has a uniform potential vorticity; 3) the flow around and below the ring is weaker than the flow of the ring; 4) the ring's intensity and amplitude are small (i.e., the ring is quasi-geostrophic); and 5) the lower layer is much deeper than the ring's amplitude. The major points of this study can be summarized as follows:

(i) The distortion of the ring is cause solely by the lower layer shear; it is independent of the (weak) upper exterior shear.

(ii) When the flow of the ring rotates in the same direction as the flow of the lower layer, the lower layer

shear elongates the ring along the lower layer flow. Hence, the elliptical ring is aligned along the lower layer flow (Figs. 3 and 6). On the other hand, when the flow of the ring rotates in the opposite sense to that of the lower layer flow, then the lower layer shear squeezes the ring along the lower layer shear. Hence, the ring is oriented across the lower layer flow (Figs. 4 and 6). When no shear exists in the lower layer, the ring's shape is circular, even though there may exist an upper exterior shear (Fig. 7). Of course, this result is only valid for our order of approximation (i.e., quasi-geostrophic motions).

(iii) When the upper exterior flow rotates in the same sense as the lower layer shear, U-turned flows are found on both sides of the ring (Fig. 3). In contrast, when the flow of the upper exterior rotates in the opposite direction to the shear of the lower layer, chains of vortices are generated on both sides of the ring (Fig. 4). These vortices decay slowly as one moves away from the ring. They are attributed to trapped planetary waves.

Possible application of the present theory to cold-core Gulf Stream rings (Fig. 8) is mentioned.

Acknowledgments. This study was supported by National Science Foundation Grant OCE-871103 and Office of Naval Research Contract N00014-87-G-0209. Discussions with Drs W. Dewar, G. Weatherly and M. E. Stern were very useful.

REFERENCES

Batchelor, G. K., 1967: *An Introduction to Fluid Dynamics.* Cambridge University Press.

Csanady, G. T., 1979: The birth and death of a warm-core ring. *J. Geophys. Res.*, **84,** 777–780.

Cushman-Roisin, B., 1986: Linear stability of large, elliptical warm-core rings. *J. Phys. Oceanogr.*, **16,** 1158–1164.

——, 1987: Exact analytical solutions for elliptical vortices of the shallow-water equations. *Tellus,* **39,** 235–244.

——, W. H. Heil and D. Nof, 1985: Oscillations and rotations of elliptical warm-core rings. *J. Geophys. Res.*, **90,** 11 756–11 764.

Flierl, G., 1979: A simple model of the structure of warm and cold-core rings. *J. Geophys. Res.*, **84,** 78–85.

——, 1987: Isolated eddy models in geophysics. *Ann. Rev. Fluid Mech.*, **19,** 493–530.

Garabedian, P. R., 1964: *Partial Differential Equations.* Wiley and Sons, 672 pp.

Hogg, N. G., 1983: Hydraulic control and flow separation in a multi-layered fluid with applications to the Vema Channel. *J. Phys. Oceanogr.*, **13,** 695–708.

Ingersoll, A. P., and P. G. Cuong, 1981: Numerical model of long-lived Jovian vortices. *J. Atmos. Sci.*, **38,** 2067–2076.

Kelley, E. A., and G. L. Weatherly, 1985: Abyssal eddies near the Gulf Stream. *J. Geophys. Res.*, **90,** 3151–3159.

Kida, S., 1981: Motion of an elliptic vortex in a uniform shear flow. *J. Phys. Soc. Japan,* **50,** 3517–3520.

Lewis, J. K., and A. D. Kirwan, 1987: Genesis of a Gulf of Mexico ring as determined from kinematic analysis. *J. Geophys. Res.*, **92,** 11 727–11 740.

McCalpin, J., 1987: On the adjustment of azimuthally perturbed vorticies. *J. Geophys. Res.*, **92,** 8213–8225.

McCartney, M. S., 1975: Inertial Taylor columns on a beta plane. *J. Fluid Mech.*, **68,** 71–95.

Melander, M. V., J. C. McWilliams and N. J. Zabusky, 1987: Axisymmetrization and vorticity-gradient intensification of an isolated two-dimensional vortex through filamentation. *J. Fluid Mech.*, **178,** 137–159.

Mied, R. P., and G. J. Lindemann, 1983: Azimuthal structure of a cyclonic Gulf Stream ring. *J. Geophys. Res.*, **88,** 2530–2546.

Milne-Thomson, L. M., 1960: *Theoretical Hydrodynamics.* Macmillan, 660 pp.

Moore, D. W., and P. G. Saffman, 1972: Structure of a line vortex in an imposed strain. *Aircraft Wake Turbulence,* J. Olsen, H. Goldburg, and A. Rogers, Eds., Plenum, 339–354.

Nof, D., 1983a: On the migration of isolated eddies with application to Gulf Stream rings. *J. Mar. Res.*, **41,** 399–425.

——, 1983b: The translation of isolated cold eddies on a sloping bottom. *Deep-Sea Res.*, **30,** 171–182.

——, 1985: On the ellipticity of isolated anticyclonic eddies. *Tellus,* **37,** 77–86.

Ruddick, B. R., 1987: Anticyclonic lenses in large scale train and shear. *J. Phys. Oceanogr.*, **17,** 741–749.

Send, U., 1986: Barotropic shear flow instability over the Continental Shelf. *1986 Summer Study Program in Geophysical Fluid Dynamics, WHOI,* WHOI-86-45, 241–250.

Shi, C., 1988: The eccentricity of warm- and cold-core rings. M.S. thesis, Florida State University, 65 pp.

Spence, T., and R. Legeckis, 1981: Satellite and hydrographic observations of low-frequency wave motions associated with a cold-core Gulf Stream ring. *J. Geophys. Res.*, **86,** 1945–1953.

Swenson, M., 1982: Isolated two-dimensional vortices in the presence of shear. *Summer Study Program in Geophysical Fluid Dynamics, WHOI,* WHOI-82-45, 324–336.

Vastano, A. C., J. E. Schmitz and D. E. Hagan, 1980: The physical oceanography of two rings observed by the Cyclonic Ring Experiment. Part I: Physical structures. *J. Geophys. Oceanogr.*, **10,** 493–513.

Young, W. R., 1986: Elliptical vortices in shallow water. *J. Fluid Mech.*, **171,** 101–119.